Synthesis of Ordered Aluminophosphate and Galloaluminophosphate Mesoporous Materials with Anion-Exchange Properties Utilizing Polyoxometalate Cluster/Surfactant Salts as Precursors

Brian T. Holland, Paul K. Isbester, Christopher F. Blanford, Eric J. Munson, and Andreas Stein*

Contribution from the Department of Chemistry, University of Minnesota, Minneapolis, Minnesota 55455

Received March 13, 1997[⊗]

Abstract: Ordered nonlamellar mesoporous aluminophosphates and galloaluminophosphates have been synthesized by introducing phosphate linking groups to cluster/surfactants salts of prearranged $AlO_4Al_{12}(OH)_{24}(H_2O)_{12}^{7+}$ (Al_{13}) and $GaO_4Al_{12}(OH)_{24}(H_2O)_{12}^{7+}$ ($GaAl_{12}$) tridecamers. The Al_{13} and $GaAl_{12}$ polyoxocations form a layered mesoscopic salt with the anionic surfactant sodium dodecylsulfate. Upon the reaction with a buffered hydrogen phosphate/dihydrogen phosphate solution the layers of clusters are transformed into a nonlayered, nearly hexagonal mesoscopic phase. Removal of the surfactant from the alumino- and galloaluminophosphates by anion-exchange results in mesoporous materials with BET surface areas up to 630 and 455 m^2/g, respectively. FT-IR and ^{27}Al and ^{31}P MAS−NMR as well as $^{27}Al \rightarrow {}^{31}P$ cross-polarization experiments indicate that the phosphate treatment results in the formation of new bonds between aluminate and phosphate species. A fraction of the clusters are transformed leading to an increase in the number of tetrahedral aluminate groups in the product. Multiple anion-exchange, e.g., with acetate, dichromate, or naphthol yellow S ions, is possible in these open mesoporous structures, which form a new class of inorganic anion-exchangers.

Introduction

Mesoporous inorganic solids containing pores in the size range between 20 and 500 Å have been studied for many years.[1] However, interest in such materials burgeoned when new methods were developed that allowed the introduction of greater order in mesoporous structures. Two different approaches, both based on surfactant-assisted ordering, have been used. One is typified by a hydrothermal reaction during which inorganic monomeric or small oligomeric precursors are assembled through cooperative interactions with surfactant molecules and subsequently condensed to form stable two- and three-dimensional networks.[2−4] In the case of silicates, this procedure results in materials of the type M41S and related hexagonal, lamellar, or cubic structures.[5] Catalytically active metals can be incorporated in the silicate structure, and pure transition metal analogs have been created.[6−13] The compositional range of mesoporous materials has been further extended by attaching organic functional groups to the channel walls, such as amine, phenyl, and vinyl groups.[14−16] A second approach is based on employing a layered starting material, such as the silicate kanemite, and transforming the stacks of silicate sheets, which are covalently connected in two dimensions, into a corrugated mesopore structure through the use of intercalated surfactant molecules. This process results in the formation of FSM-type mesoporous materials.[17,18]

Here we present a third approach toward surfactant-based mesoporous sieve synthesis that has allowed us to create for the first time ordered mesoporous aluminophosphates and galloaluminophosphates with open channels. These materials exhibit high surface areas as well as anion-exchange capabilities. The method is based on a two-step synthesis. In the first step, charged inorganic cluster precursors are prearranged as a mesoscopic salt with surfactant molecules of the opposite charge. In a second step, linking molecules are allowed to diffuse through the salt structure. Their reaction with the clusters leads to the formation of either connected cluster-linker networks or

[⊗] Abstract published in *Advance ACS Abstracts,* July 1, 1997.

(1) Behrens, P. *Adv. Mater.* **1993**, *5*, 127−132.
(2) Huo, Q.; Margolese, D. I.; Ciesla, U.; Feng, P.; Gier, T. E.; Sieger, P.; Leon, R.; Petroff, P. M.; Schüth, F.; Stucky, G. D. *Nature* **1994**, *368*, 317−321.
(3) Beck, J. S.; Vartulli, J. C.; Kennedy, G. J.; Kresge, C. T.; Roth, W. J.; Schramm, S. E. *Chem. Mater.* **1994**, *6*, 1816−1821.
(4) Huo, Q.; Margolese, D. I.; Stucky, G. D. *Chem. Mater.* **1996**, *8*, 1147−1160.
(5) Beck, J. S.; Vartuli, J. C.; Roth, W. J.; Leonowicz, M. E.; Kresge, C. T.; Schmitt, K. D.; Chu, C. T.-W.; Olson, D. H.; Sheppard, E. W.; McCullen, S. B.; Higgins, J. B.; Schlenker, J. L. *J. Am. Chem. Soc.* **1992**, *114*, 10834−10843.
(6) Corma, A.; Navarro, M. T.; Pariente-Pérez; Sánchez, F. In *Zeolites and Related Microporous Materials: State of the Art 1994*; Weitkamp, J., Karge, H. G., Pfeifer, H., Hölderich, W., Eds.; Studies in Surface Science and Catalysis 84; Elsevier Science B.V.: 1994; pp 69−75.
(7) Koyano, K. A.; Tatsumi, T. *Chem. Commun.* **1996**, 145−146.
(8) Reddy, K. M.; Moudrakovski, I.; Abdelhamid, S. *J. Chem. Soc., Chem. Commun.* **1994**, 1059−1060.
(9) Tanev, P. T.; Chibwe, M.; Pinnavaia, T. J. *Nature* **1994**, *368*, 321.
(10) Luca, V.; MacLachlan, D. J.; Hook, J. M.; Withers, R. *Chem. Mater.* **1995**, *7*, 2220−2223.
(11) Sayari, A.; Danumal, C.; Moudrakovski, I. L. *Chem. Mater.* **1995**, *7*, 813−815.
(12) Antonelli, D. M.; Nakahira, A.; Ying, J. Y. *Inorg. Chem.* **1996**, *35*, 3126−3136.
(13) Antonelli, D. M.; Ying, J. Y. *Chem. Mater.* **1996**, *8*, 874−881.
(14) Macquarrie, D. J. *Chem. Commun.* **1996**, 1961−1962.
(15) Lim, M. H; Blanford, C. F.; Stein, A. *J. Am. Chem. Soc.* **1997**, *119*, 4090−4091.
(16) Burkett, S. L.; Sims, S. D.; Mann, S. *Chem. Commun.* **1996**, 1367−1368.
(17) Inagaki, S.; Fukushima, Y.; Okada, A.; Kurauchi, T.; Kuroda, K.; Kato, C. In *Proceedings of the 9th International Zeolite Conference*; von Ballmoos, R., Ed.; Butterworth-Heinemann: Montreal, 1992; pp 305−311.
(18) Inagaki, S.; Fukushima, Y.; Kuroda, K. *J. Chem. Soc., Chem. Commun.* **1993**, 680−682.

S0002-7863(97)00823-8 CCC: $14.00

derivative-networks of the *transformed* clusters and the linkers. When the appropriate conditions are chosen, channel arrays can be created, which, upon surfactant removal, lead to high surface area mesoporous materials. As we will show in this paper, the two-step procedure is a route to certain mesoporous materials that may not be obtainable in a single-step hydrothermal synthesis, such as that of MCM-41. The method differs from the kanemite transformation by the fact that the layers of clusters typically obtained in the first step are not initially connected in the layer plane. Instead the clusters appear to be discrete entities within each layer.

Previously Stein et al. applied a similar method, the "salt-gel" synthesis to the connection of preordered niobotungstate clusters ($Nb_xW_{6-x}O_{19}^{(2+x)-}$) using silicate linkers.[19,20] Although Nb−O−Si connections were formed, resulting in mesoporous materials with surface areas up to 265 m^2/g, the final products were not ordered. Fyfe et al. were able to create lamellar, cubic, and hexagonal silicates and aluminosilicates by vapor-phase treatment of double four-ring silicate or aluminosilicate cluster anions that were prearranged in a surfactant mesostructure.[21]

Similar to silicates, aluminophosphates can form a wide array of framework structures ranging from dense quartz-like phases to open-framework zeotypes. Typical AlPO-molecular sieves are comprised of alternating AlO_4 and PO_4 tetrahedra connected by shared oxygen atoms. Both tetrahedral and octahedral aluminum units are present in aluminum metaphosphate.[22] Syntheses of aluminophosphates templated with surfactant arrays have, until now, always resulted in lamellar mesostructures.[23−25] These syntheses typically employed mixtures of alumina and phosphoric acid with a neutral alkylamine. Mesostructured alumina precipitated in the presence of anionic phosphate surfactants also adopts a lamellar structure.[2]

The mesoporous aluminophosphates and galloaluminophosphates presented here are formed by utilizing $AlO_4Al_{12}(OH)_{24}(H_2O)_{12}^{7+}$ (Al_{13}) and $GaO_4Al_{12}(OH)_{24}(H_2O)_{12}^{7+}$ ($GaAl_{12}$) polyoxocation precursors. The Al_{13} tridecamer, and more recently the $GaAl_{12}$ tridecamer, have been studied extensively as pillars for nanostructured layered materials.[26−28] The Al_{13} and $GaAl_{12}$ clusters are especially suitable precursors for the formation of porous materials because of the following properties. First, they possess a high positive charge (+7) which allows them to be templated with anionic surfactant molecules to form a layered material. Second, water and hydroxide groups associated with the tridecamers form reactive sites for direct or bridged linkages between clusters. At a certain pH these clusters condense, forming Al−OH−Al linkages between individual clusters.[29] However, connections involving silicate[30] and phosphate bridges between the Al_{13} and $GaAl_{12}$ tridecamers are also possible. As phosphate connections are made the tridecamers disintegrate into species of lower nuclearity, as indicated by solid-state ^{27}Al and ^{71}Ga MAS−NMR, and the layered phase is transformed into one that is nonlayered. Upon surfactant removal, the aluminophosphate and galloaluminophosphate mesoporous materials exhibit high surface areas, 630 and 455 m^2/g, respectively. Preliminary tests with acetate, dichromate, and naphthol yellow S anions indicate that these mesoporous structures may be useful as inorganic anion-exchange materials with ion-exchange capacities similar to hydrotalcites.

Experimental Section

Preparation of Compounds. Synthesis of the Keggin-like Ion $AlO_4Al_{12}(OH)_{24}(H_2O)_{12}^{7+}$. The Al_{13} ions were prepared in aqueous solution according to literature procedures.[31] Deionized water was used in all preparations. A 0.200 M $AlCl_3{\cdot}6H_2O$ (Aldrich) solution was base hydrolyzed by the slow addition of a 0.200 M NaOH (EM Science) solution under vigorous stirring. The final OH/Al mol ratio was ca. 2.25. The solution pH ranged from 3.9 to 4.7, depending on the rate of stirring and residual Al^{3+}.

Synthesis of the Keggin-like Ion $GaO_4Al_{12}(OH)_{24}(H_2O)_{12}^{7+}$. The $GaAl_{12}$ ions were prepared in aqueous solution according to literature procedures.[31] A 0.200 M $AlCl_3{\cdot}6H_2O$ and a 0.016 M $GaCl_3$ solution (Al:Ga = 12:1) was base hydrolyzed by the addition of a 0.200 M NaOH solution under vigorous stirring. The final OH/M mol ratio was ca. 2.22. Residual Al_{13} ions were converted to the thermally more stable $GaAl_{12}$ ions by refluxing the solution for 48 h.

Addition of Surfactant to $AlO_4Al_{12}(OH)_{24}(H_2O)_{12}^{7+}$ and $GaO_4Al_{12}(OH)_{24}(H_2O)_{12}^{7+}$. Templating of the clusters was achieved through the addition of an aqueous solution of $C_{12}H_{25}OSO_3Na$ (sodium dodecylsulfate, SDS, Aldrich) to the solution of Al_{13} or $GaAl_{12}$ tridecamers with a small excess (8:1 mole ratio) of SDS to cluster. The white precipitate, which formed immediately, was allowed to age for 1−5 min in solution before either phosphate addition or isolation by filtration. The filtered white precipitate was washed with deionized water and air dried. Calculated values for $[AlO_4Al_{12}(OH)_{24}(H_2O)_{12}^{7+}][C_{12}H_{25}OSO_3^-]_7$: 12.11 wt % Al, 34.83 wt % C, 7.77 wt % H, 7.75 wt % S; observed for a typical sample 12.71 wt % Al (24.01 wt % Al_2O_3), 37.99 wt % C, 8.00 wt % H, 8.30 wt % S, (S/Al_{13} = 7.1). The discrepancies between observed and calculated values may be due to variations in the water content and average cluster charge (pH-dependent) of the sample. The composition can also vary slightly with condensation of the clusters after aging. Calculated values for $[GaO_4Al_{12}(OH)_{24}(H_2O)_{12}^{7+}][C_{12}H_{25}OSO_3^-]_7$: 2.37 wt % Ga, 11.01 wt % Al, 34.32 wt % C, 7.65 wt % H, 7.63 wt % S; observed 2.57 wt % Ga, 10.22 wt % Al (19.31 wt % Al_2O_3), 36.37 wt % C, 7.60 wt % H, 8.07 wt % S, (S/Ga = 6.8, Al/Ga = 10.3).

Addition of Buffered Na_2HPO_4/NaH_2PO_4 Solution to an Al_{13}/SDS or $GaAl_{12}$/SDS Suspension. The Al_{13}/SDS or $GaAl_{12}$/SDS salts were stirred in a Na_2HPO_4/NaH_2PO_4 solution (Fisher) (Al/P = 1; total $[PO_4^{2-}]$ = 2.5 M) for 6 h at room temperature. The solution was originally buffered at pH = 4.25, at which the Al_{13} and $GaAl_{12}$ clusters are stable. The most ordered products were obtained if the pH was then lowered to 3 with 6 M HCl. Analysis of a typical phosphate-treated sample of the Al_{13} tridecamer: 18.95 wt % Al_2O_3, 19.93 wt % P_2O_5, 1.27 wt % Na_2O, 24.33 wt % C, 5.68 wt % H, 5.17 wt % S, (S/Al_{13} = 5.6, P/Al_{13} = 9.8, P/Al= 0.76). Average XRD d_{001} spacing for eight samples: 40.6 ± 2 Å. Analysis of a typical phosphate-treated sample of the $GaAl_{12}$ tridecamer: 18.09 wt % Al_2O_3, 16.15 wt % P_2O_5, 2.88 wt % Na_2O, 2.14 wt % Ga, 25.91 wt % C, 5.75 wt % H, 6.55 wt % S, (S/Ga = 6.7, P/Ga = 7.4, P/Al = 0.64, Al/Ga = 11.6). Average XRD d_{001} spacing for two samples: 37.6 ± 1 Å.

(19) Stein, A.; Fendorf, M.; Jarvie, T. P.; Mueller, K. T.; Benesi, A. J.; Mallouk, T. E. *Chem. Mater.* **1995**, *7*, 304−313.
(20) Stein, A.; Fendorf, M.; Jarvie, T. P.; Mueller, K. T.; Garcia, M. E.; Mallouk, T. E. In *Advances in Porous Materials*; Komarneni, S., Smith, D. M., Beck, J. S., Eds.; Mat. Res. Soc. Symp. Proc. 371; Materials Research Society: Pittsburgh, PA, 1995; pp 69−79.
(21) Fyfe, C. A.; Fu, G. *J. Am. Chem. Soc.* **1995**, *117*, 9709−9714.
(22) Pauling, L.; Sherman, J. *Z. Krist.* **1937**, *96*, 481−487.
(23) Chenite, A.; Page, Y. L.; Karra, V. R.; Sayari, A. *Chem. Commun.* **1996**, 413−414.
(24) Oliver, S.; Kuperman, A.; Coombs, N.; Lough, A.; Ozin, G. A. *Nature* **1995**, *378*, 47−50.
(25) Sayari, A.; Karra, V. R.; Reddy, J. S.; Moudrakovski, I. L. *Chem. Commun.* **1995**, 411−412.
(26) Olivera-Pastor, P.; Maireles-Torres, P.; Rodríguez-Castellón, E.; Jiménez-López, A.; Cassagneau, T.; Jones, D. J.; Rozière, J. *Chem. Mater.* **1996**, *8*, 1758−1769.
(27) Clearfield, A.; Roberts, B. D. *Inorg. Chem.* **1988**, *27*, 3237.
(28) Bradley, S. M.; Kydd, R. A. *Catal. Lett.* **1991**, *8*, 185−192.
(29) Furrer, G.; Ludwig, C.; Schindler, P. W. *J. Colloid Interfac. Sci.* **1992**, *149*, 56−67. The notation $[AlO_{4/4}]^+$ (adopted from Furrer et al.) implies that each of the four oxygen atoms in this tetrahedral group is shared by adjacent octahedral groups and contributes 1/4 to the group. $[AlO_{1/4}(OH)_{4/2}(H_2O)]^{0.5+}$ denotes an octahedral aluminum atom with one terminal water ligand, sharing one oxygen and three brigding hydroxide groups with adjacent aluminum atoms.
(30) Holland, B.; Isbester, P.; Munson, E.; Stein, A. Unpublished results.
(31) Bradley, S. M.; Kydd, R. A.; Fyfe, C. A. *Inorg. Chem.* **1992**, *31*, 1181−1185.

Surfactant Removal by Anion-Exchange with Sodium Acetate. The anionic surfactant (SDS) was removed by stirring 0.5 g of the alumino- or galloaluminophosphates in 40 mL of a 0.05 M CH_3CO_2-Na/EtOH (Aldrich) at room temperature for 20 min. The product was collected by filtration, washed with ethanol, and dried in air. Analysis of a typical extracted aluminophosphate sample: 22.82 wt % Al_2O_3, 24.47 wt % P_2O_5, 7.61 wt % Na_2O, 8.90 wt % C, 2.48 wt % H, 0.34 wt % S, ($S/Al_{13} = 0.3$, $P/Al_{13} = 10$, $P/Al = 0.77$). Average XRD d_{001} spacing for four samples: 39.0 ± 3 Å. Analysis of a typical extracted galloaluminophosphate sample: 27.63 wt % Al_2O_3, 25.42 wt % P_2O_5, 9.36 wt % Na_2O, 3.25 wt % Ga, 7.12 wt % C, 2.38 wt % H, 4.50 wt % S, ($S/Ga = 3.0$, $P/Ga = 7.7$, $P/Al = 0.66$, $Al/Ga = 11.6$). The Fourier transform infrared (FT-IR) spectrum did not show any surfactant absorptions. Average XRD d_{001} spacing for three samples: 37.0 ± 1 Å.

Other Anion Exchanges. The extracted mesoporous product was stirred for 12 h in a 0.072 mM aqueous solution of the dye naphthol yellow S (NYS^{2-}, Aldrich). Dye uptake was determined spectrophotometrically by comparing the absorption peak of the supernatant solution at $\lambda_{max} = 430$ nm to a series of standards. Uptake of NYS^{2-} was 1.6 and 1.4 meq/g for the aluminophosphate and galloaluminophosphate, respectively. A similar anion-exchange reaction was carried out with dichromate ions ($\lambda_{max} = 352$ nm; uptake: 0.16 meq/g and 0.37 meq/g for the aluminophosphate and galloaluminophosphate, respectively). The uptake of dichromate was also observed in the solid product by diffuse reflectance spectroscopy (absorptions at $\lambda_{max} = 350$, 400, and 550 nm), using a Hewlett Packard 8254A diode array spectrophotometer with a Labsphere RSA-HP-84 reflectance spectroscopy accessory.

Product Characterization. Chemical analyses for C, H, and S were carried out by Atlantic Microlab Inc., Norcross, GA. Si, Al, Ga, and P analyses were carried out by the Geochemical Lab, University of Minnesota, Minneapolis, MN. X-ray powder patterns were obtained using the Siemens D-500 Wide Angle XRD with Cu-K_α radiation. FT-IR spectra were collected with a Perkin-Elmer 1600 Series FT-IR spectrometer, using KBr pellets of the sample. N_2 adsorption measurements, utilizing BET calculations of surface area and pore size measurements, were carried out with a Micromeritics ASAP 2000 V3.00 sorption analyzer. Thermogravimetric analysis (TGA) was performed on a Perkin-Elmer TGA-7 thermal analyzer attached to a PC via a TAC7/DX thermal controller. The samples were heated under flowing nitrogen from 30 to 800 °C at 15 °C/min. Transmission electron microscopy (TEM) images were obtained on a Philips CM30 transmission electron microscope operating at 300 kV with a LaB_6 filament or on a JEOL 1210 transmission electron microscope operated at 120 kV with a tungsten filament. Images were recorded on film or using a cooled Gatan Multiscan 1k × 1k CCD array. Specimens were prepared for examination by grinding or sonicating the material in ethyl alcohol and dispersing it on a holey carbon grid. Small-angle neutron scattering (SANS) experiments were performed at the SAND beamline of the Intense Pulsed Neutron Source at Argonne National Laboratory, Argonne, IL. Samples were loaded into Suprasil cylindrical cells with a 1 mm path length. The scattered neutrons were measured using a 128 × 128 array of position sensitive, gas filled, 40 × 40 cm^2, proportional counters with the wavelengths measured by time-of-flight with data in the q range of 0.0035 to 0.8 $Å^{-1}$ taken in a single measurement.

Solution ^{27}Al NMR was performed on a Varian VXR-500 spectrometer at 130.254 MHz and referenced against an $Al(H_2O)_6^{3+}$ standard. Solid-state ^{27}Al (78.183 MHz, pulse width 5.75 μs, pulse delay 0.2 s, 2048 transients), ^{71}Ga (91.494 MHz, pulse width 8.00 μs, pulse delay 0.5 s, 5120 transients), and ^{31}P (121.336 MHz, pulse width 6.00 μs, pulse delay 60 s, 64 transients) MAS−NMR spectra (single-pulse) were collected on a Chemagnetics CMX-300 spectrometer (7.0 Tesla), with a Chemagnetics Pencil probe and a 7.5 mm zirconia rotor (7 kHz spinning rate). Solutions of 1 M $Al(H_2O)_6^{3+}$, 1 M $Ga(H_2O)_6^{3+}$, and 85% H_3PO_4 were used as external chemical shift standards. $^{27}Al \rightarrow {}^{31}P$ cross-polarization (CP) experiments were performed on a Chemagnetics CMX Infinity spectrometer operating at 162.0 MHz for ^{31}P and 104.3 MHz for ^{27}Al. In all CP experiments 80 000 transients were acquired with a 50 ms recycle delay, 0.15 ms contact time, a 16 μs 90° pulse width, and a spinning rate of 3 kHz.

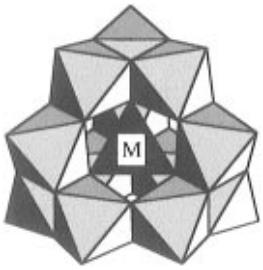

Figure 1. Schematic structure of the $AlO_4Al_{12}(OH)_{24}(H_2O)_{12}^{7+}$ and $GaO_4Al_{12}(OH)_{24}(H_2O)_{12}^{7+}$ polyoxocations, which are comprised of 12 AlO_6 octahedra surrounding a central tetrahedral MO_4 site (M = Al or Ga).

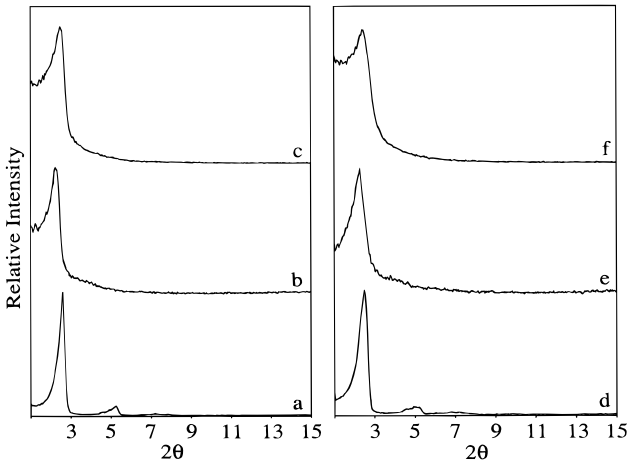

Figure 2. Powder X-ray diffraction patterns of (a) the Al_{13}/SDS salt; (b) the aluminophosphate before extraction of the surfactant; (c) the aluminophosphate after extraction of the surfactant; (d) the $GaAl_{12}$/SDS salt; (e) the galloaluminophosphate before extraction of the surfactant; and (f) the galloaluminophosphate after extraction.

Results and Discussion

The Cluster Precursors: Al_{13} and $GaAl_{12}$ Keggin-like Ions. The Al_{13} and $GaAl_{12}$ ions are structurally analogous to one of the Keggin-like ions, the Baker−Figgis ϵ-isomer, which consists of an $[AlO_{4/4}]^+$ or $[GaO_{4/4}]^+$ tetrahedral center surrounded by 12 $[AlO_{1/4}(OH)_{4/2}(H_2O)]^{0.5+}$ octahedral units (Figure 1).[29,32] The overall symmetry of these polyoxocation clusters is nearly tetrahedral. In the case of Al_{13} the fit of the central tetrahedral aluminum atom is not perfect, resulting in an inward distortion of the octahedral aluminum groups.[33] The $GaAl_{12}$ ion is a thermally more stable analog of the Al_{13} ion. The additional stability is thought to result from an increased symmetry brought upon by a better fit with the larger gallium atom.

The formation of the Al_{13} Keggin-like ion is well documented.[29,31,34,35] In solution the Al_{13} ion is stable for periods up to 6 months if the neutralization ratio $r_{OH}([OH]_{tot}/[Al(III)]_{tot})$ does not exceed the value of 2.5 and the pH is maintained below 5.[29] We found that above a pH of ca. 5.5 the Al_{13} ions began to aggregate, forming a white precipitate as a result of polymerization between the clusters.

Solution ^{27}Al NMR spectra showed a peak at 62.9 ppm due to the central tetrahedral aluminum atom, confirming the presence of the Al_{13} ion. A peak corresponding to the octahedral aluminum atoms is normally not seen in the solution spectra

(32) Baker, L. C. W.; Figgis, J. S. *J. Am. Chem. Soc.* **1970**, *92*, 3794.
(33) Johansson, G. *Acta Chem. Scand.* **1960**, *14*, 771.
(34) Bottero, J. Y.; Axelos, M.; Tchoubar, D.; Cases, J. M.; Fripiat, J. J.; Fiessinger, F. *J. Colloid Interfac. Sci.* **1987**, *117*, 47−57.
(35) Akitt, J. W.; Farthing, A. *J. Magn. Reson.* **1978**, *32*, 345−352.

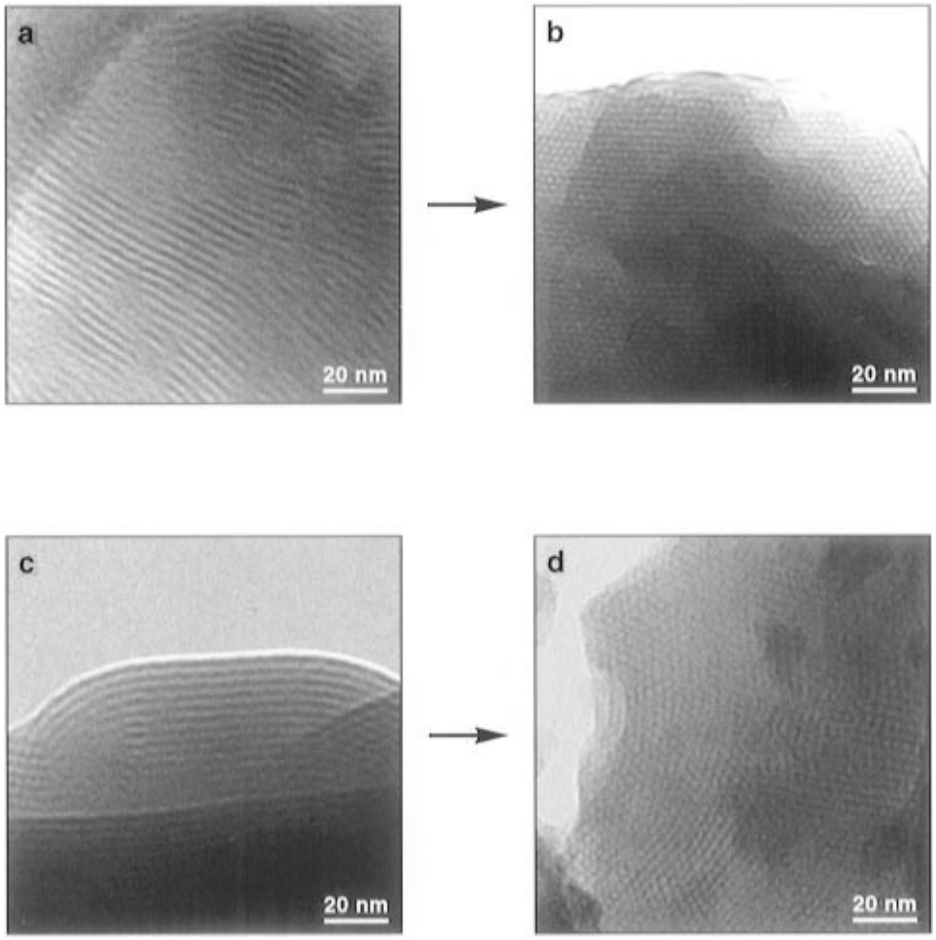

Figure 3. Transmission electron micrographs of (a) the Al_{13}/SDS salt, showing the lamellar mesostructure of alternating Al_{13} cluster/surfactant layers; (b) the extracted aluminophosphate exhibiting a mesopore channel structure; (c) the $GaAl_{12}$/SDS salt; and (d) the extracted galloaluminophosphate. An approximate scale bar is shown.

due to excessive broadening of the distorted octahedral groups.[36] In contrast, an Al_{Oh} peak can be seen in the ^{27}Al MAS−NMR spectrum of the $GaAl_{12}$ solution at 9 ppm, due to the increased symmetry in that species.[31]

Arranging the Clusters as Al_{13} and $GaAl_{12}$/Surfactant Salts. The Al_{13} and $GaAl_{12}$ tridecamers carry a charge of +7. They readily precipitate as ordered salts with anionic surfactants, including sodium dodecyl sulfate (SDS), cetylphosphate, and dodecyl benzene sulfonic acid (DBSA). Figure 2a shows the XRD powder pattern of the white Al_{13}/SDS salt, with a set of d_{001}, d_{002}, and d_{003} reflections, typical for a layered material with a basal spacing of ca. 34.5 Å. A layered structure is also observed in the $GaAl_{12}$/SDS salt with a d_{001} basal-spacing of ca. 35.3 Å (Figure 2d). The layering can be seen in the transmission electron micrographs of both the Al_{13}/SDS and $GaAl_{12}$/SDS salts (Figure 3 (parts a and c)). The cluster/surfactant superstructure is controlled by electrostatic interactions between the clusters and the polar head groups of the surfactant molecules, together with hydrophobic interactions among the surfactant tails. The structure of amphiphilic liquid-crystal arrays as well as surfactant/inorganic phases has previously been related to the ratio $g = V/(a_o l)$, where V is the total volume of the surfactant chains, a_o is the effective head group area at a micelle surface, and l is the kinetic surfactant tail length.[4,37] In the present case the high charge density on the inorganic clusters is partially screened by the surfactant charges, resulting in a large enough ratio of chain-volume to head-group-area for layering ($0.5 < g < 1.0$). Lamellar phases have been frequently observed with cationic precursors and anionic surfactants.[2] The approximate surfactant layer thickness can be estimated from the difference between the layer spacing and the diameter of the Al_{13} ion (∼9−10 Å).[19] The resulting value of ca. 25−26 Å indicates that the SDS molecules form interpenetrating bilayers (the extended length of SDS is ca. 19 Å).

These layer structures are different from those in surfactant-intercalated kanemite. In the kanemite/surfactant complex each inorganic layer consists of an "infinite" sheet of covalently bonded silicate units. In the cluster/surfactant salts, the inorganic layers appear to be composed mainly of distinct clusters that are not interconnected. FT-IR spectra of the Al_{13}/SDS salts exhibited the fingerprint of intact Al_{13} cluster ions in the solid (absorption bands at 727, 628, 546, and 493 cm^{-1}), and the C, H, S analyses were most consistent with the composition $[AlO_4Al_{12}(OH)_{24}(H_2O)_{12}^{7+}]$ $[C_{12}H_{25}OSO_3^-]_7$. The ^{27}Al MAS−NMR spectrum showed resonances for tetrahedral AlO_4 at a chemical shift of 61.0 ppm and for octahedral AlO_6 units at ca. −3.0 ppm (Figure 4a). The signal for octahedral Al, which was absent in solution, is very intense in the solid state. This effect has been previously observed in pillared clays and has been explained by the large quadrupolar interaction of the ^{27}Al nucleus, which leads to rapid nuclear relaxation and signal broadening via the lifetime-broadening mechanism. For instrumental reasons, broad solution signals usually cannot be observed when much narrower resonances are also present.[38] The presence of intact $GaAl_{12}$ clusters in the $GaAl_{12}$/SDS

(36) Kunwar, A. C.; Thompson, A. R.; Gutowsky, H. S.; Oldfield, E. J. *J. Magn. Reson.* **1984**, *60*, 467.
(37) Gruner, S. M. *J. Phys. Chem.* **1989**, *93*, 7562.

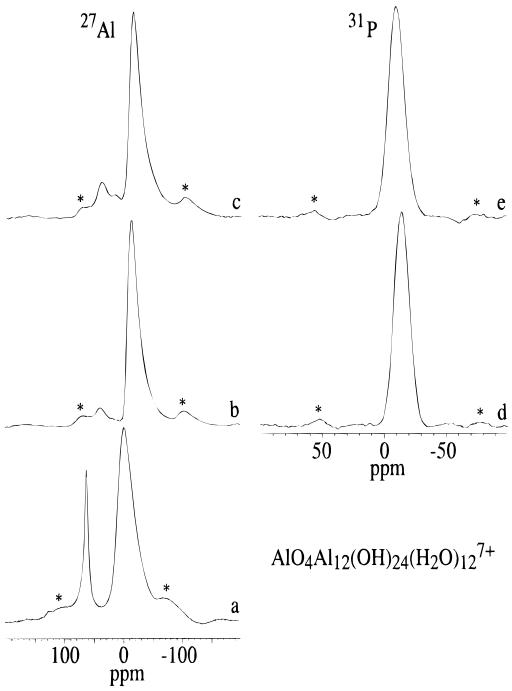

Figure 4. Multinuclear solid-state NMR spectra of the structures based on the Al_{13} clusters: (a) the Al_{13}/SDS salt (^{27}Al); (b) and (d) the phosphate-treated sample (^{27}Al and ^{31}P, respectively); (c) and (e) the product after extraction of the surfactant (^{27}Al and ^{31}P, respectively). The asterisks denote spinning sidebands.

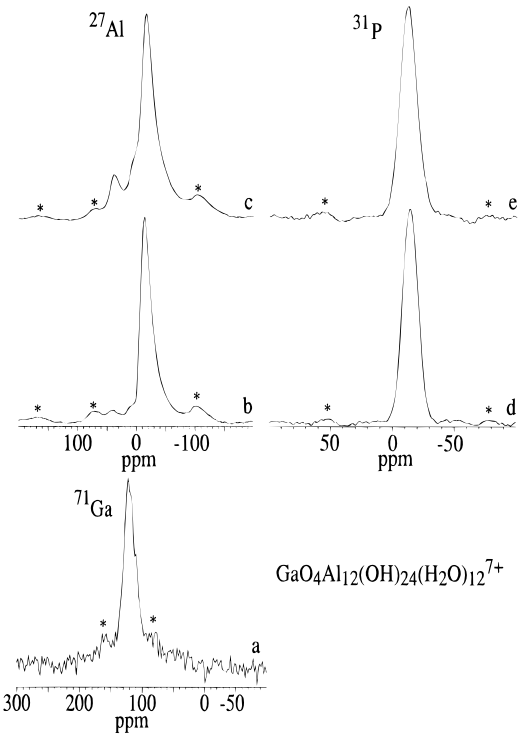

Figure 5. Multinuclear solid-state NMR spectra of the structures based on the $GaAl_{12}$ clusters: (a) the $GaAl_{12}$/SDS salt (^{71}Ga); (b) and (d) the phosphate-treated sample (^{27}Al and ^{31}P, respectively); (c) and (e) the product after extraction of the surfactant (^{27}Al and ^{31}P, respectively). The asterisks denote spinning sidebands.

samples was also confirmed by FT-IR spectroscopy. Absorption bands were observed at 703, 622, 544, and 494 cm^{-1}. The ^{71}Ga MAS−NMR spectrum showed a resonance for tetrahedral GaO_4 with a chemical shift of ca. 123.0 ppm (Figure 5a). As expected, the only resonance present in ^{27}Al MAS−NMR spectrum of $GaAl_{12}$/SDS was attributed to octahedral aluminum from the tridecamer with a chemical shift of ca. 8 ppm.

Small-angle neutron scattering (SANS) experiments were carried out to further probe the layer structure. Small-angle scattering can be analyzed by using the Guinier approximation, which is described by

$$I(q) = NV^2(\Delta\rho)^2 \exp(-q^2R_g^2/3)$$

where N is the number of particles, V the particle volume, $(\Delta\rho)$ the difference in the scattering length density of the particle and any solvent present, R_g the radius of gyration, and q the wave vector (which is related to the d-spacing via $q = 2\pi/d$).[39] The variation of the intensity with the scattering angle in the small-angle scattering region (Guinier region) can be described by various power laws, with exponents that are characteristic for a given geometry. Layered materials typically display a power law q-dependence of $I(q) \sim 1/q^2$. The layer thickness can be derived from SANS data. For "infinitely" large sheets with a finite thickness, it is given by $R_t \cdot \sqrt{12}$, where R_t is derived from the modified Guinier law for sheets

$$I(q) \propto 1/q^2 \exp(-q^2R^2_t)$$

Figure 6 is a log I vs log q SANS plot for a dry sample of Al_{13}/SDS. Within experimental uncertainty the peak at q = 0.17 $Å^{-1}$ is consistent with the interlayer distance obtained from the d_{001} peak in the XRD. Very little intensity is found in the Guinier region, so that a reliable Guinier analysis could not be carried out. The low intensity is consistent with the presence of individual cluster ions that are too small (less than 10 Å thick) to observe any correlation by SANS. Larger aggregates of clusters would result in a significant small-angle scattering intensity.

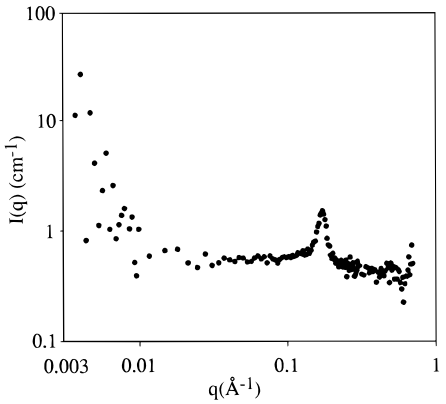

Figure 6. log I vs log q SANS plot for the Al_{13}/SDS salt.

Addition of a Na_2HPO_4/NaH_2PO_4 Buffer Solution to an Al_{13}/SDS and $GaAl_{12}$/SDS Suspension. In order to link the Al_{13} clusters within the salt structure, the Al_{13}/SDS salt was stirred in a Na_2HPO_4/NaH_2PO_4 solution that was buffered at pH = 4.25, at which the Al_{13} clusters are stable. However, the best products were obtained if the pH was then lowered with HCl solution. The reaction of the Al_{13}/SDS salt with phosphate was manifested in several ways. The surfactant:aluminum ratio was reduced from ca. 0.55−0.43. The layered material was transformed into a nonlayered mesostructure, as shown by a single low-angle d_{001} XRD peak at ca. 39 Å for a typical sample and no distinctive higher order peaks (Figure 2b). The ^{27}Al

(38) Anderson, M. W.; Klinowski, J. *Inorg. Chem.* **1990**, *29*, 3260−3263.

(39) Carrado, K. A.; Thiyagarajan, P.; Winans, R. E.; Botto, R. E. *Inorg. Chem.* **1991**, *30*, 794−799.

MAS−NMR spectrum (Figure 4b) displays two broad resonances, a weak peak centered at 39.5 ppm and an intense peak at −14.0 ppm. The characteristic peak at 61.0 ppm due to tetrahedral aluminum occupying the core of a Keggin-like cluster is absent. The new resonance at 39.5 ppm is diagnostic for tetrahedral aluminum surrounded by four tetrahedral phosphate groups, which has been reported to fall in the range from 35 to 48 ppm for microporous aluminophosphates.[40] Our results therefore suggest that a significant fraction of the clusters has disintegrated during the reaction with phosphate groups. The peak corresponding to octahedral aluminum at −14.0 ppm has also shifted upfield compared to the untreated Al_{13}/SDS salt. It has been reported that the chemical shift of octahedral aluminum varies nearly linearly with the number of phosphate groups in its coordination shell over the range from 0 ppm for $Al(H_2O)_6^{3+}$ to −18 ppm for $Al(PO_4)_6$ units in aluminum metaphosphate.[40] The upfield shift of the Al_{Oh} resonance after phosphate-treatment of the Al_{13}/SDS salt indicates that Al−O−P bonds have indeed formed, leading to an increased shielding of the Al_{Oh}. The broadness of the resonances can be attributed to quadrupolar coupling in a distribution of local environments. The quadrupolar coupling effect makes it difficult to quantify the relative ratios of Al_{Td} and Al_{Oh}.[41]

The ^{31}P spectrum of the phosphate-treated material displayed a large broad peak at ca. −14 ppm vs 85% H_3PO_4 (Figure 4d). ^{31}P chemical shifts for $P(OAl)_4$ environments in $AlPO_4$ materials are normally between −23 and −35 ppm and shift to higher frequency in $AlPO_4$ materials containing higher coordinated aluminum.[42] Based on the measured chemical shifts, the connections in our materials appear to involve individual tetrahedral PO_4 groups linked mostly to octahedral aluminum atoms. Similar bonds between tetrahedral phosphate and octahedral aluminate are observed in aluminum metaphosphate, variscite, and metavariscite.[43−45] The broadness of the peak in Figure 4d again results from a distribution of local P environments, including contributions from connections between tetrahedral Al and phosphate groups. The shift is outside the range typically observed for P−O−P linkages.[40,46] The absence of P−O−P linkages, together with the measured mole ratio of 10 P/Al_{13}, support the conclusion that clusters are no longer intact, since fewer attachment sites for phosphate would be expected in Al_{13} clusters.

The disintegration of the Al_{13} tridecamer is believed to be due to the change in the hydrolysis ratio r_{OH}. When the pH is lowered from ca. 4.3 to 3, r_{OH} decreases from 2.2 to less than 0.5.[47] In solution the main species present at this low value are monomeric aluminum species of the type $Al(H_2O)_6^{3+}$, $Al(H_2O)_5(OH)^{2+}$, and $Al(H_2O)_4(OH)_2^{+}$. Within the surfactant salt structure similar units can be expected. Without lowering the pH to ca. 3 with HCl, the reaction products tended to be very disordered and surfactant removal was difficult.

The $GaAl_{12}$/SDS salt behaved in a manner similar to the Al_{13}/SDS salt, undergoing a transformation from a layered to a nonlayered material with the addition of a phosphate solution. The d_{001} low-angle peak in the XRD powder pattern shifted to 38.4 Å and the higher-angle layer peaks disappeared (Figure 2e). The ^{27}Al MAS−NMR spectrum indicates the presence of a tetrahedral and two octahedral aluminum sites with resonances at 40.4, 8.8, and −11.5 ppm, respectively (Figure 5b). The appearance of an Al_{Td} peak proves that at least some clusters have disintegrated, as the $GaAl_{12}$/SDS salt contained no tetrahedral aluminum. During breakdown of the $GaAl_{12}$ cluster some of the Al_{Oh} is transformed into Al_{Td}, probably as a result of the acid addition and subsequent formation of monomeric species. The MAS ^{31}P NMR spectrum displays a broad peak similar to the aluminophosphate (Figure 5d). The MAS ^{71}Ga NMR spectrum did not show a distinct signal for this quadrupolar nucleus, due to the increase in gallium environments and a decrease in symmetry of the gallium sites compared to the original $GaAl_{12}$ clusters.

During phosphate treatment two effects can contribute to the phase change from a lamellar to a hexagonal structure. First, upon acid addition some of the clusters break into smaller fragments which carry a lower positive charge per fragment than the original Al_{13} clusters. Secondly, the negative phosphate groups "neutralize" some of the positive charges on the polyoxocations. Thus they decrease the charge density of the inorganic aluminophosphate region as well as the ratio of chain-volume to head-group-area of the surfactant assembly. This results in an increased curvature of the inorganic-surfactant interface and the concomitant transformation from a lamellar to a hexagonal phase. The behavior is similar to that described by Fyfe and Fu for silicate polyanions.[21]

Aluminophosphate zeotypes typically exhibit lower thermal and hydrothermal stabilities than silicate- and aluminosilicate-based zeolites.[48,49] These characteristics also apply to the mesoporous aluminophosphate, compared to silicate mesoporous sieves. Calcination of the aluminophosphate/SDS composite at temperatures between 350 and 540 °C resulted in collapse of the structure. Thermogravimetric analysis (TGA) combined with chemical analysis indicated that during heating the samples first lost all their water by 135 °C, then the hydrocarbon component of the surfactant by 340−360 °C, and finally the sulfate component (as SO_2), which remained in the samples after the hydrocarbon tail of the surfactant had been removed. The final residue of the aluminophosphate at 770 °C exhibited the dense tridymite structure. Mesoporosity could, however, be achieved by extraction of the surfactant from the uncalcined materials.

Surfactant Extraction of the Metallophosphate/SDS Composite. The surfactant was extracted by anion-exchange of the aluminophosphate/SDS composite with an ethanol/sodium acetate solution. The extraction was complete after stirring 20 min at room temperature. Surfactant removal resulted in a mesoporous aluminophosphate with a BET surface area of 630 m^2/g and a pore volume of 0.40 cm^3/g. The pore size distribution curve showed a narrow range of pore diameters in the small mesopore range (<30 Å, peaking at 17 Å) with no evidence for any larger pores. The relatively regular order of the extracted product was also evident from the TEM image (Figure 3b) and further manifested itself by a slight increase in the intensity of the low-angle XRD peak at $d_{001} = 38$ Å (Figure 2c). Even after the extraction process, infrared absorptions characteristic for the Al_{13} were present (slightly shifted adsorption peaks at 635 and 545 cm^{-1}, shoulders at ca. 725 and 485 cm^{-1}), indicating that some of the clusters remained intact. However, the ^{27}Al MAS−NMR spectrum of the extracted

(40) Sayari, A.; Moudrakovski, I.; Reddy, J. S.; Ratcliffe, C. I.; Ripmeester, J. A.; Preston, K. F. *Chem. Mater.* **1996**, *8*, 2080−2088.
(41) Engelhardt, G.; Michel, D. *High-Resolution Solid-State NMR of Silicates and Zeolites*; John Wiley and Sons Ltd.: Norwich, 1987.
(42) Barrie, P. J. *NMR Applications to Porous Solids*; Barrie, P. J., Ed., 1995; Vol. 30, pp 37−91.
(43) van der Meer, H. *Acta Cryst.* **1976**, *B32*, 2423−2426.
(44) Kniep, R.; Mootz, D. *Acta Cryst.* **1973**, *B29*, 2292−2294.
(45) Kniep, R.; Mootz, D. *Acta Cryst.* **1977**, *B33*, 263−265.
(46) Mudrakovskii, I. L.; Shmachkova, V. P.; Kotsarenko, N. S.; Mastikhin, V. M. *J. Phys. Chem. Solids* **1986**, *47*, 335−339.
(47) Bottero, J. Y.; Cases, J. M.; Fiessinger, F.; Poirier, J. E. *J. Phys. Chem.* **1980**, *84*, 2933−2939.
(48) Hampson, B.; Leach, H. F.; Lowe, B. M.; Williams, C. D. *Zeolites* **1989**, *9*, 521−525.
(49) Choudhary, V. R.; Akolekar, D. B.; Singh, A. P.; Sansare, S. D. *J. Catal.* **1988**, *111*, 254−263.

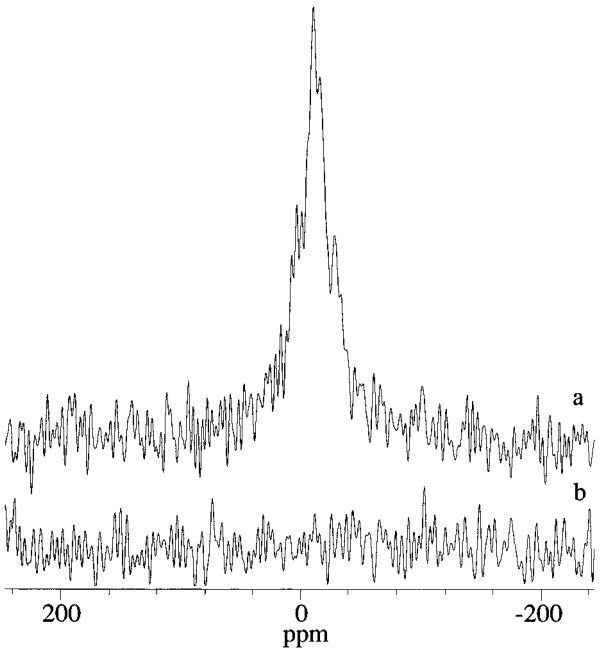

Figure 7. $^{27}Al \rightarrow {}^{31}P$ cross-polarization experiments: (a) standard cross-polarization experiment and (b) null experiment with no ^{27}Al spin lock.

material (Figure 4c) suggests that the fraction of intact clusters is low. Except for a weak new peak at 17.2 ppm, the spectrum is similar to the corresponding one before extraction, indicating that the aluminum environments changed very little upon surfactant removal, and most clusters disintegrated in the previous phosphate-treatment step. The new peak falls in the region that has been assigned to pentacoordinate aluminum, in structures where adjacent Al atoms share a hydroxide bridge.[50] The ^{31}P MAS spectrum of the extracted material displayed a large broad peak at ca. −14 ppm vs 85% H_3PO_4 (Figure 4e), as before the extraction.

In order to confirm the existence of Al−O−P bonds in this material, two experiments were performed. Figure 7a shows the results of a standard cross polarization experiment as described by Fyfe, Mueller et al.[51] A signal corresponding to phosphorus next to aluminum is clearly seen. The weak signal intensity is likely due to the short contact time used (0.15 ms) because of rapid ^{27}Al $T_{1\rho}$ relaxation times. Figure 7b shows the results of a null experiment, which was exactly the same as the previous experiment, except no ^{27}Al spin lock was applied during the cross polarization time. Ideally, no signal should be observed during the null experiment, and none was observed. Other null experiments with no ^{27}Al 90° pulse but with ^{27}Al spin lock also showed no signal. These results clearly demonstrate the presence of ^{27}Al-^{31}P dipolar interactions such as those found in Al−O−P bonds.

Surfactant extraction was also possible in case of the galloaluminophosphate/SDS composite. However, this sample behaved very differently from the corresponding aluminophosphate. While the FT-IR spectrum showed no evidence for remaining surfactant after anion-exchange with acetate ions, the sulfur analysis indicated that nearly half of the original sulfur was still present. It appears that the surfactant tail was cleaved from the sulfate head-group by acid hydrolysis in the presence of the gallium species. The mechanism of this cleavage process is not yet fully understood, but the different behavior observed for the two samples may be related to the greater acid strength of OH-groups attached to gallium compared to those attached to aluminum.[52] The low-angle peak in the XRD shifted to a *d*-spacing of 36.8 Å (Figure 2f). The ^{27}Al MAS−NMR spectrum showed the presence of both tetrahedral and octahedral aluminum typical for aluminophosphates, at 40.6 and −13.3 ppm, respectively, and a shoulder at 7.3 ppm, which is in the region for octahedral aluminum of the $GaAl_{12}$ tridecamer (Figure 5c). The MAS ^{31}P NMR spectrum again displayed a broad peak at −11.2 ppm (Figure 5e), and no MAS ^{71}Ga NMR resonances were observable due to broadening effects. The TEM image displays a nearly hexagonal order similar to that of MCM-41 (Figure 3d). Nitrogen adsorption measurements indicate a BET surface area of 455 m^2/g with a pore volume of 0.37 cm^3/g and a narrow pore size distribution similar to the mesoporous aluminophosphate, peaking at 18 Å.

It is interesting to note that water loss occurred at a higher temperature in the extracted samples than in the surfactant-containing materials (225 °C for the aluminophosphate; 175−310 °C for the galloaluminophosphate). Both samples still displayed a low-angle XRD peak after heating in nitrogen at 200 °C for 1 h (d_{001} = 31 Å for the aluminophosphate and 33 Å for the galloaluminophosphate). For the extracted galloaluminophosphate, water loss occurred over two regions; nearly half of the water was removed by 175 °C and the second half by 310 °C. The water released at the higher temperature is likely to be associated with octahedral aluminum sites near a remaining sulfate group. In the corresponding aluminophosphate sample, a very weak peak present in the derivative TGA curve below 300 °C may also be associated with water on Al_{Oh} near a remaining sulfate group. For comparison, in basic aluminum sulfate, the Al_{13} tridecamer units gradually lose their water and hydroxyl groups over the range from 80 to 360 °C.[53] In those materials the sulfate oxygen atoms are known to be involved in hydrogen bonding.[54]

Ion-Exchange Properties. The ion-exchange properties of the cluster-based alumino- and galloaluminophosphates are noteworthy. Both anionic and cationic charge-balancing groups are associated with this network, and both may be exchangeable. The cation exchange sites involve Na^+ ions or protons that balance the single remaining charge on phosphate groups linking aluminum species. The anion exchange sites result from the high positive charge on the cluster which is originally balanced by the anionic surfactant template, SDS. While a number of inorganic cation exchange materials (such as zeolites) exist, few inorganic anion exchangers can be found. Hydrotalcite clays comprise one such class of materials.[55] We tested the anion exchange properties of the mesoporous alumino- and galloaluminophosphate by removing the surfactant with sodium acetate (first anion-exchange) and then stirring the surfactant-extracted material for 12 h in an 0.072 mM aqueous solution of naphthol yellow S (NYS^{2-}) (second anion-exchange). The dye uptake was measured by comparing the 430 nm absorption of the supernatant to a series of standards. The measured NYS^{2-} uptake of 1.6 and 1.4 meq/g for the alumino- and galloaluminophosphate samples, respectively, is comparable to the ion-exchange capacities of anion-exchange resins and hydrotalcites. A similar anion-exchange reaction was also possible with dichromate ions, but the uptake was smaller. Studies are now

(50) Pluth, J. J.; Smith, J. V.; Bennett, J. M. *Acta Cryst.* **1986**, *C42*, 283−286.
(51) Fyfe, C. A.; Mueller, K. T.; Grondey, H.; Wong-Moon, K. C. *J. Phys. Chem.* **1993**, *97*, 13484−13495.
(52) Wade, K. D.; Banister, A. J. In *Comprehensive Inorganic Chemistry*; Bailar, J. C., Emeléus, H. J., Nyholm, R., Trotman-Dickenson, A. F., Eds.; Vol. 1, Pergamon Press: Oxford, 1973; p 1071.
(53) Kloprogge, J. T.; Geus, J. W.; Jansen, J. B. H.; Seykens, D. *Thermochim. Acta* **1992**, *209*, 265−276.
(54) Johansson, G. *Acta Chem. Scand.* **1962**, *16*, 403−420.
(55) Cavani, F.; Trifirò, F.; Vaccari, A. *Catal. Today* **1991**, *11*, 171−291.

underway to further quantify and optimize the exchange properties of this new class of ion-exchange materials.

Conclusion

This study has shown that nearly-hexagonally ordered mesoporous metallophosphates can be readily synthesized by a two-step synthesis involving the formation of cluster-surfactant salts in the first step, followed by a phosphate linking step. The clusters break up during the linking reaction, forming a network of $Al_{Oh}-O-P_{Td}$ linkgages, as well as a fraction of tetrahedral aluminum sites. The resulting surface areas are high and comparable to MCM-41 type aluminosilicates. This procedure was successfully demonstrated for aluminophosphate and galloaluminophosphate systems, but further compositional variations are possible. We are presently studying systems based on chromium, manganese, iron, and pure gallium polyoxocation clusters[56−58] to incorporate paramagnetic or catalytically active components in the mesoporous structures. We have also carried out a similar reaction of an Al_{13}/SDS salt with silicate links and obtained high surface area products.[30]

The synthetic method presented here provides an alternative approach to the synthesis of mesoporous materials, where the direct hydrothermal reaction of a metal oxide precursor in surfactant solution does not lead to three-dimensional mesoporous structures. The anion-exchange capabilities of these materials may extend the range of potential uses for mesoporous materials to new types of chromatographic, catalytic, and host−guest applications.

Acknowledgment. A.S. thanks 3M, the David and Lucille Packard Foundation, the Donors of the Petroleum Research Fund, administered by the American Chemical Society, and the Office of the Vice President for Research and Dean of the Graduate School of the University of Minnesota for support of this research. This work has benefited from the use of the Intense Pulsed Neutron Source at Argonne National Laboratory. This facility is funded by the U.S. Department of Energy, BES-Materials Science, under Contract W-31-109-Eng-38. The authors acknowledge the assistance of P. Thiyagarajan (IPNS) with the SANS experiment. B.H. and C.F.B. gratefully acknowledge the Center for Interfacial Engineering at the University of Minnesota for CIE-NSF graduate fellowships.

Supporting Information Available: Pore size distribution curves for the extracted aluminophosphate and galloaluminophosphate, TGA and derivative TGA curves, and XRD powder patterns of the extracted aluminophosphate and galloaluminophosphate after heating under nitrogen at 200 °C for 1 h (9 pages). See any current masthead pages for ordering and Internet access instructions.

JA970823X

(56) Bradley, S. M.; Lehr, C. R.; Kydd, R. A. *J. Chem. Soc., Dalton Trans.* **1993**, 2415−2420.

(57) Bradley, S. M.; Kydd, R. A. *J. Chem. Soc., Dalton Trans.* **1993**, 2407−2413.

(58) Kudynska, J.; Buckmaster, H. A.; Kawano, K.; Bradley, S. M.; Kydd, R. A. *J. Chem. Phys.* **1993**, *99*, 3329−3334.